Published in final edited form as:
J Med Chem. 2013 November 14; 56(21): . doi:10.1021/jm4012356.

Effects of Amino Acids on Melanoma Targeting and Clearance Properties of Tc-99m-Labeled Arg-X-Asp-Conjugated α-Melanocyte Stimulating Hormone Peptides

Adam M. Flook[†], **Jianquan Yang**[†], and **Yubin Miao**[*,†,‡,§]

[†]College of Pharmacy, University of New Mexico, Albuquerque, NM 87131, USA.

[‡]Cancer Research and Treatment Center, University of New Mexico, Albuquerque, NM 87131, USA.

[§]Department of Dermatology, University of New Mexico, Albuquerque, NM 87131, USA.

Abstract

The purpose of this study was to examine the effects of amino acids on melanoma targeting and clearance properties of new ^{99m}Tc-labeled Arg-X-Asp-conjugated alpha-melanocyte stimulating hormone (α-MSH) peptides. RSD-Lys-(Arg^{11})CCMSH {c[Arg-Ser-Asp-$_D$Tyr-Asp]-Lys-Cys-Cys-Glu-His-$_D$Phe-Arg-Trp-Cys-Arg-Pro-Val-NH_2}, RNleD-Lys-(Arg^{11})CCMSH, RPheD-Lys-(Arg^{11})CCMSH and R$_D$PheD-Lys-(Arg^{11})CCMSH peptides were synthesized and evaluated for their melanocortin-1 (MC1) receptor binding affinities in B16/F1 melanoma cells. The biodistribution of ^{99m}Tc-RSD-Lys-(Arg^{11})CCMSH, ^{99m}Tc-RFD-Lys-(Arg^{11})CCMSH and ^{99m}Tc-RfD-Lys-(Arg^{11})CCMSH were determined in B16/F1 melanoma-bearing C57 mice. The substitution of Gly with Ser, Phe and $_D$Phe increased the MC1 receptor binding affinities of the peptides, whereas the substitution of Gly with Nle decreased the MC1 receptor binding affinity of the peptide. ^{99m}Tc-RSD-Lys-(Arg^{11})CCMSH exhibited the highest melanoma uptake (18.01 ± 4.22% ID/g) and the lowest kidney and liver uptake among these ^{99m}Tc-peptides. The B16/F1 melanoma lesions could be clearly visualized by SPECT/CT using ^{99m}Tc-RSD-Lys-(Arg^{11})CCMSH as an imaging probe. It is desirable to reduce the renal uptake of ^{99m}Tc-RSD-Lys-(Arg^{11})CCMSH to facilitate its potential therapeutic application.

Keywords

Alpha-melanocyte stimulating hormone peptide; receptor-targeting; melanoma imaging

INTRODUCTION

Malignant melanoma is the most lethal form of skin cancer with an increasing incidence.[1] Unfortunately, no curative treatment exists for metastatic melanoma. It is of great interest to develop receptor-targeting imaging probes for melanoma. Both melanocortin-1 (MC1) and $\alpha_v\beta_3$ integrin receptors have been attractive molecular targets for developing melanoma imaging probes.[2-22] Generally, the radiolabeled α-melanocyte stimulating hormone (α-MSH) peptides could target the MC1 receptors,[2-14] whereas the radiolabeled Arg-Gly-Asp (RGD) peptides could bind to the $\alpha_v\beta_3$ integrin [15-22] receptors. In 2010, we reported a novel α-MSH hybrid peptide which could target both MC1 and $\alpha_v\beta_3$ integrin receptors.[23]

[*]**Corresponding Author** phone, 505-925-4437; ymiao@salud.unm.edu..

The authors declare no competing financial interest.

Specifically, a cyclic RGD motif {Arg-Gly-Asp-DTyr-Asp} was attached to [Cys^{3,4,10}, D-Phe^{7}, Arg^{11}]α-MSH$_{3-13}$ peptide via a lysine linker to yield RGD-Lys-(Arg^{11})CCMSH peptide. The dual receptor-targeting ^{99m}Tc-RGD-Lys-(Arg^{11})CCMSH displayed enhanced melanoma uptake as compared to single receptor-targeting ^{99m}Tc-RAD-Lys-(Arg^{11})CCMSH or ^{99m}Tc-RGD-Lys-(Arg^{11})CCMSH$_{scramble}$ in M21 human melanoma-xenografts.[23] Interestingly, the substitution of Gly in ^{99m}Tc-RGD-Lys-(Arg^{11})CCMSH with Ala, Thr and Val improved the MC1 receptor binding affinities and enhanced the melanoma uptake in B16/F1 melanoma-bearing C57 mice.[23-25] These interesting findings suggested that the single amino acid at that specific position generated a profound impact on the MC1 receptor binding affinity.

The structural differences among Gly, Ala, Thr and Val were minimal. As compared to Gly, the Ala has one extra -CH_3 group, the Thr has one extra -$CH(OH)CH_3$ group, whereas the Val has one extra -$CH(CH_3)_2$ group. The comparison in biodistribution results of ^{99m}Tc-RXD-Lys-(Arg^{11})CCMSH (X = Gly, Ala, Thr and Val) demonstrated that such subtle structural modification retained high melanoma uptake in B16/F1 melanoma-bearing C57 mice. Thus, we were interested in whether and how other amino acids could affect the melanoma targeting and pharmacokinetic properties of ^{99m}Tc-RXD-Lys-(Arg^{11})CCMSH peptide. For instance, whether and how a long hydrocarbon chain and a bulky benzene ring could affect the receptor binding and melanoma targeting properties of the peptides. In this study, we replaced the Gly with Ser, Nle, Phe and DPhe to generate four new peptides, namely RSD-Lys-(Arg^{11})CCMSH, RNleD-Lys-(Arg^{11})CCMSH, RFD-Lys-(Arg^{11})CCMSH and RfD-Lys-(Arg^{11})CCMSH peptides. The MC1 receptor binding affinities of these four peptides were examined in B16/F1 melanoma cells. Based on the receptor binding affinities, we further radiolabeled RSD-Lys-(Arg^{11})CCMSH, RFD-Lys-(Arg^{11})CCMSH and RfD-Lys-(Arg^{11})CCMSH with ^{99m}Tc. Then we determined the cellular internalization and efflux in B16/F1 melanoma cells and biodistribion properties in B16/F1 melanoma-bearing C57 mice for these three ^{99m}Tc-peptides. Thereafter, we determined the imaging property of ^{99m}Tc-RSD-Lys-(Arg^{11})CCMSH in B16/F1 melanoma-bearing C57 mice.

RESULTS

The schematic structures of RSD-Lys-(Arg^{11})CCMSH, RNleD-Lys-(Arg^{11})CCMSH, RFD-Lys-(Arg^{11})CCMSH and RfD-Lys-(Arg^{11})CCMSH are presented in Figure 1. The peptides were synthesized and purified by reverse phase-high performance liquid chromatography (RP-HPLC). The overall synthetic yields were 30% for all four peptides. The chemical purities of RSD-Lys-(Arg^{11})CCMSH, RNleD-Lys-(Arg^{11})CCMSH, RFD-Lys-(Arg^{11})CCMSH and RfD-Lys-(Arg^{11})CCMSH were greater than 95% after the HPLC purification. The peptide identities were confirmed by electrospray mass spectrometry (MS). The measured molecular weight was 2180 for RSD-Lys-(Arg^{11})CCMSH, 2206 for RNleD-Lys-(Arg^{11})CCMSH, 2240 for RFD-Lys-(Arg^{11})CCMSH and RfD-Lys-(Arg^{11})CCMSH. The competitive binding curves of the peptides are shown in Figure 2. The IC_{50} value was 1.30 ± 0.36 nM for RSD-Lys-(Arg^{11})CCMSH, 2.99 ± 0.26 nM for RNleD-Lys-(Arg^{11})CCMSH, 0.82 ± 0.06 nM for RFD-Lys-(Arg^{11})CCMSH, and 1.35 ± 0.08 nM for RfD-Lys-(Arg^{11})CCMSH in B16/F1 melanoma cells, respectively.

Because RNleD-Lys-(Arg^{11})CCMSH exhibited lowest receptor binding affinity among four peptides, as well as lower receptor binding affinity than that of RGD-Lys-(Arg^{11})CCMSH in our previous report,[26] we only further evaluated the other three peptides. RSD-Lys-(Arg^{11})CCMSH, RFD-Lys-(Arg^{11})CCMSH and RfD-Lys-(Arg^{11})CCMSH were readily radiolabeled with ^{99m}Tc with greater than 95% radiolabeling yields. All three ^{99m}Tc-peptides were separated from their excess non-labeled peptides by RP-HPLC. The radiochemical purities of three ^{99m}Tc-peptides were greater than 99% (Table 1). The

specific activities of ^{99m}Tc-RSD-Lys-(Arg^{11})CCMSH, ^{99m}Tc-RFD-Lys-(Arg^{11})CCMSH and ^{99m}Tc-RfD-Lys-(Arg^{11})CCMSH were 8.834 × 10^9, 8.598 × 10^9 , 8.598 × 10^9 MBq/g, respectively. The retention times of ^{99m}Tc-RSD-Lys-(Arg^{11})CCMSH, ^{99m}Tc-RFD-Lys-(Arg^{11})CCMSH and ^{99m}Tc-RfD-Lys-(Arg^{11})CCMSH were 12.5, 18.4 and 20.8 min, respectively. ^{99m}Tc-RSD-Lys-(Arg^{11})CCMSH, ^{99m}Tc-RFD-Lys-(Arg^{11})CCMSH and ^{99m}Tc-RfD-Lys-(Arg^{11})CCMSH were stable in mouse serum at 37°C for 24 h (Figure 3). Cellular internalization and efflux properties of ^{99m}Tc-RSD-Lys-(Arg^{11})CCMSH, ^{99m}Tc-RFD-Lys-(Arg^{11})CCMSH and ^{99m}Tc-RfD-Lys-(Arg^{11})CCMSH were examined in B16/F1 cells. Figure 4 illustrates the internalization and efflux properties of ^{99m}Tc-RSD-Lys-(Arg^{11})CCMSH, ^{99m}Tc-RFD-Lys-(Arg^{11})CCMSH and ^{99m}Tc-RfD-Lys-(Arg^{11})CCMSH. All three ^{99m}Tc-peptides exhibited rapid cellular internalization and prolonged cellular retention. Approximately 69% of ^{99m}Tc-RSD-Lys-(Arg^{11})CCMSH, 87% of ^{99m}Tc-RFD-Lys-(Arg^{11})CCMSH and 87% of ^{99m}Tc-RfD-Lys-(Arg^{11})CCMSH activities were internalized in the cells after 20 min of incubation. Cellular efflux results indicated that 76% of ^{99m}Tc-RSD-Lys-(Arg^{11})CCMSH, 73% of ^{99m}Tc-RFD-Lys-(Arg^{11})CCMSH and 46% of ^{99m}Tc-RfD-Lys-(Arg^{11})CCMSH activities remained inside the cells after 2 h of incubation in the culture medium.

The melanoma targeting and pharmacokinetic properties of ^{99m}Tc-RSD-Lys-(Arg^{11})CCMSH, ^{99m}Tc-RFD-Lys-(Arg^{11})CCMSH and ^{99m}Tc-RfD-Lys-(Arg^{11})CCMSH are shown in Tables 2-4. Both ^{99m}Tc-RFD-Lys-(Arg^{11})CCMSH and ^{99m}Tc-RfD-Lys-(Arg^{11})CCMSH exhibited similar tumor uptake pattern in B16/F1 melanoma-bearing C57 mice. ^{99m}Tc-RFD-Lys-(Arg^{11})CCMSH exhibited its highest tumor uptake of 15.01 ± 4.40% ID/g at 4 h post-injection, whereas ^{99m}Tc-RfD-Lys-(Arg^{11})CCMSH reached its highest tumor uptake of 13.11 ± 1.21% ID/g at 4 h post-injection. The tumor uptake values of ^{99m}Tc-RFD-Lys-(Arg^{11})CCMSH and ^{99m}Tc-RfD-Lys-(Arg^{11})CCMSH decreased to 7.19 ± 1.02 and 6.29 ± 1.39% ID/g by 24 h post-injection. The tumor blocking studies revealed that co-injection of 10 μg (6.1 nM) of non-radiolabeled NDPMSH with ^{99m}Tc-RFD-Lys-(Arg^{11})CCMSH or ^{99m}Tc-RfD-Lys-(Arg^{11})CCMSH decreased their tumor uptake values to 2.82 ± 0.48 and 1.57 ± 0.48% ID/g at 2 h post-injection, demonstrating that the tumor uptake was MC1 receptor-mediated. ^{99m}Tc-RSD-Lys-(Arg^{11})CCMSH displayed a different tumor uptake pattern as compared to ^{99m}Tc-RFD-Lys-(Arg^{11})CCMSH and ^{99m}Tc-RfD-Lys-(Arg^{11})CCMSH. ^{99m}Tc-RSD-Lys-(Arg^{11})CCMSH exhibited rapid and high melanoma uptake of 18.01 ± 4.22% ID/g at 30 min post-injection. The tumor uptake of ^{99m}Tc-RSD-Lys-(Arg^{11})CCMSH gradually reduced to 8.04 ± 1.80% ID/g at 24 h post-injection. Furthermore, co-injection of 10 μg (6.1 nM) of non-radiolabeled NDP-MSH with ^{99m}Tc-RSD-Lys-(Arg^{11})CCMSH decreased their tumor uptake value to 2.35 ± 0.01% ID/g at 2 h post-injection, demonstrating that the tumor uptake was MC1 receptor-mediated.

Kidneys were the excretion pathways for ^{99m}Tc-RSD-Lys-(Arg^{11})CCMSH, ^{99m}Tc-RFD-Lys-(Arg^{11})CCMSH and ^{99m}Tc-RfD-Lys-(Arg^{11})CCMSH. The renal uptake values of ^{99m}Tc-RSD-Lys-(Arg^{11})CCMSH, ^{99m}Tc-RFD-Lys-(Arg^{11})CCMSH and ^{99m}Tc-RfD-Lys-(Arg^{11})CCMSH were 80.01 ± 15.67, 88.08 ± 9.31 and 111.54 ± 10.19% ID/g at 2 h post injection, respectively. At 24 h post-injection, The renal uptake values of for ^{99m}Tc-RSD-Lys-(Arg^{11})CCMSH, ^{99m}Tc-RFD-Lys-(Arg^{11})CCMSH and ^{99m}Tc-RfD-Lys-(Arg^{11})CCMSH decreased to 23.15 ± 2.94, 51.01 ± 3.62 and 73.05 ± 9.87% ID/g, respectively. Liver uptake was different among these three ^{99m}Tc-peptides. ^{99m}Tc-RSD-Lys-(Arg^{11})CCMSH demonstrated lower liver uptake than ^{99m}Tc-RFD-Lys-(Arg^{11})CCMSH and ^{99m}Tc-RfD-Lys-(Arg^{11})CCMSH. The liver uptake of ^{99m}Tc-RSD-Lys-(Arg^{11})CCMSH, ^{99m}Tc-RFD-Lys-(Arg^{11})CCMSH and ^{99m}Tc-RfD-Lys-(Arg^{11})CCMSH were 1.22 ± 0.12, 9.87 ± 1.26 and 5.29 ± 1.30% ID/g at 2 h post injection, respectively.

^{99m}Tc-RSD-Lys-(Arg^{11})CCMSH exhibited faster whole-body clearance than ^{99m}Tc-RFD-Lys-(Arg^{11})CCMSH and ^{99m}Tc-RfD-Lys-(Arg^{11})CCMSH. Approximately 68% of ^{99m}Tc-RSD-Lys-(Arg^{11})CCMSH cleared through the urinary system by 2 h post-injection, whereas approximately 43% of ^{99m}Tc-RFD-Lys-(Arg^{11})CCMSH and 44% of ^{99m}Tc-RfD-Lys-(Arg^{11}) CCMSH washed through the urinary system by 2 h post-injection. At 24 h post-injection, 84% of ^{99m}Tc-RSD-Lys-(Arg^{11})CCMSH, 76% of ^{99m}Tc-RFD-Lys-(Arg^{11})CCMSH and 73% of ^{99m}Tc-RfD-Lys-(Arg^{11})CCMSH cleared out the body. ^{99m}Tc-RSD-Lys-(Arg^{11})CCMSH also displayed lower normal organ uptake than ^{99m}Tc-RFD-Lys-(Arg^{11})CCMSH and ^{99m}Tc-RfD-Lys-(Arg^{11})CCMSH. Normal organ uptake of ^{99m}Tc-RSD-Lys-(Arg^{11})CCMSH was minimal (<1.2% ID/g) except for the kidneys after 2 h post-injection.

Since ^{99m}Tc-RSD-Lys-(Arg^{11})CCMSH showed higher tumor uptake and faster urinary clearance than ^{99m}Tc-RFD-Lys-(Arg^{11})CCMSH and ^{99m}Tc-RfD-Lys-(Arg^{11})CCMSH, the effect of *L*-lysine co-injection on the tumor and renal uptake of ^{99m}Tc-RSD-Lys-(Arg^{11})CCMSH was examined in B16/F1 melanoma-bearing C57 mice. *L*-lysine co-injection significantly (*$p<0.05$) reduced the renal uptake of ^{99m}Tc-RSD-Lys-(Arg^{11})CCMSH by 37% at 2 h post-injection without affecting the tumor uptake (Figure 5). Whole-body single photon emission computed tomography (SPECT)/CT image at 2 h post-injection are presented in Figure 6. Flank B16/F1 melanoma lesions were clearly visualized by SPECT using ^{99m}Tc-RSD-Lys-(Arg^{11})CCMSH peptide as an imaging probe. The SPECT image of tumor accurately matched its anatomical location obtained in the CT image. The SPECT image showed high contrast of tumor to normal organ except for kidneys, which was consistent with the biodistribution results. The urinary metabolites of ^{99m}Tc-RSD-Lys-(Arg^{11})CCMSH at 2 h post-injection are shown in Figure 7. Approximately 70% of ^{99m}Tc-RSD-Lys-(Arg^{11})CCMSH remained intact in the urine at 2 h post-injection, while 30% of the ^{99m}Tc-RSD-Lys-(Arg^{11})CCMSH was transformed to a more hydrophobic compound.

DISCUSSION

In our previous reports,[24-26] we have found the important role of Gly in the tumor targeting property of ^{99m}Tc-RGD-Lys-(Arg^{11})CCMSH in B16/F1 melanoma-bearing C57 mice. Despite the minimal structural differences among Gly, Ala, Thr and Val amino acids, the replacement of Gly in RGD-Lys-(Arg^{11})CCMSH with Ala, Thr and Val enhanced the MC1 receptor binding affinities and B16/F1 melanoma uptake of the peptides.[24-26] In this study, we further investigated whether the substitution of Gly with a longer hydrocarbon chain (Nle) and a bulky benzene ring (Phe or $_D$Phe) could affect the receptor binding and melanoma targeting properties of the peptides. On the other hand, we hypothesized that the replacement of Gly with Ser would facilitate the urinary clearance of the peptide as compared to hydrophobic Nle, Phe and $_D$Phe. Thus, we synthesized and evaluated RSD-Lys-(Arg^{11})CCMSH, RNleD-Lys-(Arg^{11})CCMSH, RFD-Lys-(Arg^{11})CCMSH and RfD-Lys-(Arg^{11})CCMSH peptides in this study.

The introduction of Ser, Nle, Phe and $_D$Phe generated different impact on the MC1 receptor binding affinities of the peptides. The linear long hydrocarbon chain from Nle decreased the MC1 receptor binding affinity of the peptide, whereas the short CH_2OH group from Ser and the bulky benzene ring from Phe and $_D$Phe increased the MC1 receptor binding affinity of the peptides. Among these four new peptides, RNleD-Lys-(Arg^{11})CCMSH displayed the weakest MC1 receptor binding affinity of 2.99 ± 0.26 nM, whereas RSD-Lys-(Arg^{11})CCMSH and RfD-Lys-(Arg^{11})CCMSH exhibited similar strong MC1 receptor binding affinities of 1.30 ± 0.36 and 1.35 ± 0.08 nM. Overall, RfD-Lys-(Arg^{11})CCMSH showed the strongest MC1 receptor binding affinity of 0.82 ± 0.06 nM. Despite that the -His-$_D$Phe-Arg-Trp- motif is the binding moiety to MC1 receptor, the difference in receptor

binding affinity indicated that the Ser, Nle, Phe and DPhe interacted with the receptor binding moiety. Such subtle interactions were likely related to the flexibility of lactam bonds among amino acid residues in the peptides. In our previous report, [25, 26] the MC1 receptor binding affinities were 2.1, 0.3, 0.7 and 1.0 nm for RGD-Lys-(Arg^{11})CCMSH, RAD-Lys-(Arg^{11})CCMSH, RTD-Lys-(Arg^{11})CCMSH and RVD-Lys-(Arg^{11})CCMSH in B16/F1 cells, respectively. Clearly, RNleD-Lys-(Arg^{11})CCMSH displayed the weakest MC1 receptor binding affinity among all RXD-Lys-(Arg^{11})CCMSH peptides. Thus, we further radiolabeled RSD-Lys-(Arg^{11})CCMSH, RFD-Lys-(Arg^{11})CCMSH and RfD-Lys-(Arg^{11})CCMSH with ^{99m}Tc and evaluated their cellular internalization and efflux properties, as well as their in vivo biodistribution and clearance properties. It is worthwhile to note that three cysteine residues in each peptide provide a NS_3 chelating system for ^{99m}Tc. It was reported that non-radioactive rhenium-conjugated (Arg^{11})CCMSH retained comparable nanomolar MC1 receptor binding affinity as (Arg^{11})CCMSH peptide (1.9 vs. 1.7 nM). [27] Accordingly, the radiolabeling of three RXD-Lys-(Arg^{11})CCMSH peptides with ^{99m}Tc should retain their nanomolar binding affinities.

^{99m}Tc-RSD-Lys-(Arg^{11})CCMSH, ^{99m}Tc-RFD-Lys-(Arg^{11})CCMSH and ^{99m}Tc-RfD-Lys-(Arg^{11})CCMSH exhibited similar rapid internalization and prolonged efflux properties in B16/F1 melanoma cells. Despite the similar pattern in cellular internalization and efflux properties, ^{99m}Tc-RSD-Lys-(Arg^{11})CCMSH displayed a different tumor uptake pattern as compared to ^{99m}Tc-RFD-Lys-(Arg^{11})CCMSH and ^{99m}Tc-RfD-Lys-(Arg^{11})CCMSH. ^{99m}Tc-RSD-Lys-(Arg^{11})CCMSH exhibited rapid and high melanoma uptake of 18.01 ± 4.22% ID/g at 30 min post-injection. Meanwhile, ^{99m}Tc-RSD-Lys-(Arg^{11})CCMSH displayed lower renal uptake than ^{99m}Tc-RFD-Lys-(Arg^{11})CCMSH and ^{99m}Tc-RfD-Lys-(Arg^{11})CCMSH. The renal uptake of ^{99m}Tc-RSD-Lys-(Arg^{11})CCMSH was 45% of the renal uptake of ^{99m}Tc-RFD-Lys-(Arg^{11})CCMSH, and 32% of the renal uptake of ^{99m}Tc-RfD-Lys-(Arg^{11})CCMSH at 24 h post-injection. Not surprisingly, ^{99m}Tc-RSD-Lys-(Arg^{11})CCMSH also showed lower liver uptake than ^{99m}Tc-RFD-Lys-(Arg^{11})CCMSH and ^{99m}Tc-RfD-Lys-(Arg^{11})CCMSH. The liver uptake of ^{99m}Tc-RSD-Lys-(Arg^{11})CCMSH was 12% of the liver uptake of ^{99m}Tc-RFD-Lys-(Arg^{11})CCMSH, and 23% of the liver uptake of ^{99m}Tc-RfD-Lys-(Arg^{11})CCMSH at 2 h post-injection. Furthermore, ^{99m}Tc-RSD-Lys-(Arg^{11})CCMSH exhibited faster urinary clearance than ^{99m}Tc-RFD-Lys-(Arg^{11})CCMSH and ^{99m}Tc-RfD-Lys-(Arg^{11})CCMSH. Interestingly, the stereochemistry of Phe and DPhe affected the renal and liver uptake. ^{99m}Tc-RFD-Lys-(Arg^{11})CCMSH displayed higher liver uptake than that of ^{99m}Tc-RfD-Lys-(Arg^{11})CCMSH, whereas ^{99m}Tc-RfD-Lys-(Arg^{11})CCMSH displayed higher renal uptake than that of ^{99m}Tc-RFD-Lys-(Arg^{11})CCMSH. Clearly, the tumor targeting and clearance properties of ^{99m}Tc-RSD-Lys-(Arg^{11})CCMSH were more favorable than those of ^{99m}Tc-RFD-Lys-(Arg^{11})CCMSH and ^{99m}Tc-RfD-Lys-(Arg^{11})CCMSH.

The B16/F1 melanoma lesions could be clearly visualized by SPECT/CT using ^{99m}Tc-RSD-Lys-(Arg^{11})CCMSH as an imaging probe. However, the image also indicated very high renal uptake. In fact, extremely high renal uptake (67-135% ID/g at 2 h post-injection) appears to be a common issue for all reported ^{99m}Tc-RXD-Lys-(Arg^{11})CCMSH peptides. [24-26] Despite that ^{99m}Tc-RSD-Lys-(Arg^{11})CCMSH exhibited the second lowest renal uptake (80.01 ± 15.67% ID/g at 2 h post-injection) among all reported ^{99m}Tc-RXD-Lys-(Arg^{11})CCMSH peptides, it is desirable to reduce the non-specific renal uptake in future studies to facilitate its potential therapeutic application. In this study, *L*-lysine co-injection significantly (*$p<0.05$) reduced the renal uptake of ^{99m}Tc-RSD-Lys-(Arg^{11})CCMSH by 37% at 2 h post-injection without affecting its tumor uptake. Obviously, *L*-lysine co-injection can be utilized to decrease the renal uptake of ^{99m}Tc-RSD-Lys-(Arg^{11})CCMSH in future studies. The effect of *L*-lysine co-injection also highlighted the contribution of the overall positive charge of ^{99m}Tc-RSD-Lys-(Arg^{11})CCMSH to its renal uptake. Clearly, the substitution of the positively-charged Lys linker with a neutral or

negatively-charged amino acid (i.e. Gly or Glu) can decrease the overall charge of ^{99m}Tc-RSD-Lys-(Arg^{11})CCMSH. According to the effect of *L*-lysine co-injection in this study, it is very likely that the substitution of Lys with a neutral or negatively-charged amino acid will decrease the renal uptake.

CONCLUSIONS

In summary, the substitution of Gly with Ser, Phe and $_D$Phe increased the MC1 receptor binding affinities of the peptides, whereas the substitution of Gly with Nle decreased the MC1 receptor binding affinity of the peptide in B16/F1 melanoma cells. ^{99m}Tc-RSD-Lys-(Arg^{11})CCMSH exhibited higher melanoma uptake and lower kidney and liver uptake than those of ^{99m}Tc-RFD-Lys-(Arg^{11})CCMSH and ^{99m}Tc-RfD-Lys-(Arg^{11})CCMSH. The B16/F1 melanoma lesions could be clearly visualized by SPECT/CT using ^{99m}Tc-RSD-Lys-(Arg^{11})CCMSH as an imaging probe. It is desirable to reduce the non-specific renal uptake of ^{99m}Tc-RSD-Lys-(Arg^{11})CCMSH to facilitate its potential therapeutic application.

EXPERIMENTAL SECTION

Chemicals and Reagents

Amino acids and resin were purchased from Advanced ChemTech Inc. (Louisville, KY) and Novabiochem (San Diego, CA). ^{125}I-Tyr^2-[Nle^4, $_D$Phe^7]-α-MSH {^{125}I-(Tyr^2)-NDP-MSH} was obtained from PerkinElmer, Inc. (Waltham, MA) for receptor binding assay. ^{99m}TcO$^-_4$ was purchased from Cardinal Health (Albuquerque, NM). *L*-lysine was purchased from Sigma-Aldrich (St. Louis, MO). All other chemicals used in this study were purchased from Thermo Fischer Scientific (Waltham, MA) and used without further purification. B16/F1 murine melanoma cells were obtained from American Type Culture Collection (Manassas, VA).

Peptide Synthesis and *In Vitro* Competitive Binding Assay

The RSD-Lys-(Arg^{11})CCMSH, RNleD-Lys-(Arg^{11})CCMSH, RFD-Lys-(Arg^{11})CCMSH and RfD-Lys-(Arg^{11})CCMSH peptides were synthesized using fluorenylmethyloxycarbonyl (Fmoc) chemistry according to our previously published procedure[26] with slight modification on Sieber amide resin by an Advanced ChemTech multiple-peptide synthesizer (Louisville, KY). Briefly, 70 μmol of Sieber amide resin and 210 μmol of Fmoc-protected amino acids were used for the synthesis. Fmoc-Lys(Boc) was used to generate a Lys linker in each peptide. Intermediate scaffolds of H_2N-Arg(Pbf)-Ser/Nle/Phe/$_D$Phe-Asp(OtBu)-$_D$Tyr(tBu)-Asp(O-2-phenylisopropyl)-Lys(Boc)-Cys(Trt)-Cys(Trt)-Glu(OtBu)-His(Trt)-$_D$Phe-Arg(Pbf)-Trp(Boc)-Cys(Trt)-Arg(Pbf)-Pro-Val were synthesized on Sieber amide resin. The protecting group of 2-phenylisopropyl of each scaffold was removed and each peptide was cleaved from the resin treating with a mixture of 2.5% of trifluoroacetic acid (TFA) and 5% of triisopropylsilane. After the precipitation with ice-cold ether and characterization by MS, each protected peptide was dissolved in H_2O/CH_3CN (50:50) and lyophilized to remove the reagents such as TFA and triisopropylsilane. Each protected peptide was further cyclized by coupling the carboxylic group from the Asp with the alpha amino group from the Arg at the N-terminus. The cyclization reaction was achieved by overnight reaction in dimethylformamide (DMF) using benzotriazole-1-yl-oxy-tris-pyrrolidino-phosphonium-hexafluorophosphate (PyBOP) as a coupling agent in the presence of N,N-diisopropylethylamine (DIPEA). The protecting groups were totally removed by treating with a mixture of TFA, thioanisole, phenol, water, ethanedithiol and triisopropylsilane (87.5:2.5:2.5:2.5:2.5:2.5) for 2 h at room temperature (25 °C). Each peptide was precipitated and washed with ice-cold ether for four times, purified by RP-HPLC and characterized by MS. The chemical purity of each peptide was determined by

Waters RP-HPLC (Milford, MA) on a Grace Vydac C-18 reverse phase analytic column (Deerfield, IL) using a 20-min gradient of 16-26% acetonitrile in 20 mM HCl aqueous solution at a flow rate of 1 mL/min. The purities of all four peptides were greater than 95%.

The IC_{50} values of RSD-Lys-(Arg^{11})CCMSH, RNleD-Lys-(Arg^{11})CCMSH, RFD-Lys-(Arg^{11})CCMSH and RfD-Lys-(Arg^{11})CCMSH peptides for the MC1 receptor were determined in B16/F1 melanoma cells. The receptor binding assay was replicated in triplicate for each peptide. The B16/F1 cells were seeded into a 24-well cell culture plate at a density of 2.5×10^5 cells/well and incubated at 37° C overnight. After being washed with binding medium {modified Eagle's medium with 25 mM N-(2-hydroxyethyl)-piperazine-N′-(2-ethanesulfonic acid) (HEPES), pH 7.4, 0.2% bovine serum albumin (BSA), 0.3 mM 1,10-phenathroline}, the cells were incubated at 25 °C for 2 h with approximately 30,000 counts per minute (cpm) of ^{125}I-(Tyr^2)-NDP-MSH in the presence of increasing concentrations (10^{-13} M to 10^{-6} M) of each peptide in 0.3 mL of binding medium. The reaction medium was aspirated after the incubation. The cells were rinsed twice with 0.5 mL of ice-cold pH 7.4, 0.2% BSA/0.01 M phosphate buffered saline (PBS) to remove any unbound radioactivity and lysed in 0.5 mL of 1 M NaOH for 5 min. The activities associated with the cells were measured in a Wallac 2480 automated gamma counter (PerkinElmer, NJ). The IC_{50} value for each peptide was calculated using Prism software (GraphPad Software, La Jolla, CA).

Peptide Radiolabeling

Because RNleD-Lys-(Arg^{11})CCMSH exhibited lowest receptor binding affinity among four peptides, we only further evaluated the other three peptides. RSD-Lys-(Arg^{11})CCMSH, RFD-Lys-(Arg^{11})CCMSH and RfD-Lys-(Arg^{11})CCMSH peptides were labeled with ^{99m}Tc via a direct reduction reaction with $SnCl_2$. Briefly, 10 μL of 1 mg/mL $SnCl_2$ in 0.1 M HCl, 40 μL of 0.5 M NH_4OAc (pH 5.2), 100 μL of 0.2 M Na_2tartate (pH 9.2), 100 μL of fresh $^{99m}TcO_4^-$ solution (37-74 MBq), and 10 μL of 1 mg/mL of each peptide in aqueous solution were added into a reaction vial and incubated at 25 °C for 20 min to form ^{99m}Tc-labeled peptide. Each ^{99m}Tc-peptide was purified to a single species by Waters RP-HPLC (Milford, MA) on a Grace Vydac C-18 reverse phase analytic column (Deerfield, IL) using a 20-min gradient of 16-26% acetonitrile in 20 mM HCl aqueous solution at a flow rate of 1 mL/min. Each purified peptide was purged with N_2 gas for 20 min to remove the acetonitrile. The pH of final peptide solution was adjusted to 7.4 with 0.1 N NaOH and sterile normal saline for stability, biodistribution and imaging studies. The serum stabilities of ^{99m}Tc-RSD-Lys-(Arg^{11})CCMSH, ^{99m}Tc-RFD-Lys-(Arg^{11})CCMSH and ^{99m}Tc-RfD-Lys-(Arg^{11})CCMSH were determined by incubation in mouse serum at 37 °C for 24 h and monitored for degradation by RP-HPLC. Briefly, 100 μL of HPLC-purified peptide solution (~7.4 MBq) was added into 100 μL of mouse serum (Sigma-Aldrich Corp, St. Louis, MO) and incubated at 37 °C for 24 h. After the incubation, 200 μL of a mixture of ethanol and acetonitrile (V:V = 1:1) was added to precipitate the serum proteins. The resulting mixture was centrifuged at 16,000 g for 5 min to collect the supernatant. The supernatant was purged with N_2 gas for 30 min to remove the ethanol and acetonitrile. The resulting sample was mixed with 500 μL of water and injected into RP-HPLC for analysis using the gradient described above.

Cellular Internalization and Efflux

Cellular internalization and efflux of ^{99m}Tc-RSD-Lys-(Arg^{11})CCMSH, ^{99m}Tc-RFD-Lys-(Arg^{11})CCMSH and ^{99m}Tc-RfD-Lys-(Arg^{11})CCMSH were evaluated in B16/F1 melanoma cells. The B16/F1 cells were seeded into a 24-well cell culture plate at a density of 2.5×10^5 cells/well and incubated at 37° C overnight. After being washed twice with binding medium [modified Eagle's medium with 25 mM *N*-(2-hydroxyethyl)-piperazine-*N'*-(2-ethanesulfonic

acid), pH 7.4, 0.2% bovine serum albumin (BSA), 0.3 mM 1,10-phenathroline], the B16/F1 cells were incubated at 25°C for 20, 40, 60, 90 and 120 min (n=3) in the presence of approximate 300,000 counts per minute (cpm) of HPLC-purified of ^{99m}Tc-RSD-Lys-(Arg^{11})CCMSH, ^{99m}Tc-RFD-Lys-(Arg^{11})CCMSH or ^{99m}Tc-RfD-Lys-(Arg^{11})CCMSH. After incubation, the reaction medium was aspirated and the cells were rinsed with 2 × 0.5 mL of ice-cold pH 7.4, 0.2% BSA / 0.01 M PBS. Cellular internalization was assessed by washing the cells with acidic buffer [40 mM sodium acetate (pH 4.5) containing 0.9% NaCl and 0.2% BSA] to remove the membrane-bound radioactivity. The remaining internalized radioactivity was obtained by lysing the cells with 0.5 mL of 1 N NaOH for 5 min. Membrane-bound and internalized activities were counted in a gamma counter. Cellular efflux was determined by incubating the B16/F1 cells with ^{99m}Tc-RSD-Lys-(Arg^{11})CCMSH, ^{99m}Tc-RFD-Lys-(Arg^{11})CCMSH or ^{99m}Tc-RfD-Lys-(Arg^{11})CCMSH for 2 h at 25°C, removing non-specific-bound activity with 2 × 0.5 mL of ice-cold PBS rinse, and monitoring radioactivity released into cell culture medium. At time points of 20, 40, 60, 90 and 120 min, the radioactivities on the cell surface and inside the cells were separately collected and counted in a gamma counter.

Biodistribution Studies

All the animal studies were conducted in compliance with Institutional Animal Care and Use Committee approval. The biodistribution properties of ^{99m}Tc-RSD-Lys-(Arg^{11})CCMSH, ^{99m}Tc-RFD-Lys-(Arg^{11})CCMSH and ^{99m}Tc-RfD-Lys-(Arg^{11})CCMSH were determined in B16/F1 melanoma-bearing C57 female mice (Harlan, Indianapolis, IN). Each C57 mouse was subcutaneously inoculated on the right flank with 1×10^6 B16/F1 cells. The weight of tumors reached approximately 0.2 g 10 days post cell inoculation. Each melanoma-bearing mouse was injected with 0.037 MBq of ^{99m}Tc-RSD-Lys-(Arg^{11})CCMSH, ^{99m}Tc-RFD-Lys-(Arg^{11})CCMSH or ^{99m}Tc-RfD-Lys-(Arg^{11})CCMSH via the tail vein. Groups of 4 mice were sacrificed at 0.5, 2, 4 and 24 h post-injection, and tumors and organs of interest were harvested, weighed and counted. Blood values were taken as 6.5% of the body weight. The specificity of tumor uptake was determined by co-injecting ^{99m}Tc-RSD-Lys-(Arg^{11})CCMSH, ^{99m}Tc-RFD-Lys-(Arg^{11})CCMSH or ^{99m}Tc-RfD-Lys-(Arg^{11})CCMSH with 10 μg (6.1 nmol) of unlabeled NDP-MSH at 2 h post-injection.

L-lysine co-injection is effective in decreasing the renal uptake of radiolabeled α-MSH peptides. Because ^{99m}Tc-RSD-Lys-(Arg^{11})CCMSH exhibited the highest tumor uptake and fastest urinary clearance among three ^{99m}Tc-peptdes, we only examined the effect of *L*-lysine co-injection on the renal uptake of ^{99m}Tc-RSD-Lys-(Arg^{11})CCMSH. Briefly, a group of 4 mice were injected with a mixture of 0.037 MBq of ^{99m}Tc-RSD-Lys-(Arg^{11})CCMSH and 15 mg of *L*-lysine. The mice were sacrificed at 2 h post-injection, and tumors and organs of interest were harvested, weighed and counted in a gamma counter.

Melanoma Imaging with ^{99m}Tc-RSD-Lys-(Arg^{11})CCMSH

^{99m}Tc-RSD-Lys-(Arg^{11})CCMSH was the lead peptide due to its higher tumor uptake and faster urinary clearance. Thus, we further determined the melanoma imaging property of ^{99m}Tc-RSD-Lys-(Arg^{11})CCMSH. Approximately 4.1 MBq of ^{99m}Tc-RSD-Lys-(Arg^{11})CCMSH was injected into a B16/F1 melanoma-bearing C57 mouse via the tail vein. The mouse was euthanized for small animal SPECT/CT (Nano-SPECT/CT®, Bioscan, Washington DC) imaging 2 h post-injection. The 9-min CT imaging was immediately followed by the SPECT imaging of whole-body. The SPECT scans of 24 projections were acquired. Reconstructed data from SPECT and CT were visualized and co-registered using InVivoScope (Bioscan, Washington DC).

Urinary Metabolites of ^{99m}Tc-RSD-Lys-(Arg^{11})CCMSH

We also examined the urinary metabolites of ^{99m}Tc-RSD-Lys-(Arg^{11})CCMSH. Approximately 3.7 MBq of ^{99m}Tc-RSD-Lys-(Arg^{11})CCMSH was injected into a B16/F1 melanoma-bearing C57 mouse via the tail vein to determine the urinary metabolites. The mouse was euthanized to collect urine at 2 h post-injection. The collected urine sample was centrifuged at 16,000 g for 5 min before the HPLC analysis. Thereafter, an aliquot of the urine was injected into the HPLC. A 20-minute gradient of 16-26% acetonitrile / 20 mM HCl with a flow rate of 1 mL/min was used for urine analysis.

Statistical Analysis

Statistical analysis was performed using the Student's t-test for unpaired data to determine the significance of differences in tumor and kidney uptake with/without peptide blockade or with/without *L*-lysine co-injection in biodistribution studies described above. Differences at the 95% confidence level ($p<0.05$) were considered significant.

Acknowledgments

We appreciate Dr. Fabio Gallazzi for his technical assistance.This work was supported in part by the NIH grant NM-INBRE P20RR016480/P20GM103451 and UNM RAC Award. The images were generated by the KUSAIR established with funding from the W.M. Keck Foundation and the UNM Cancer Research and Treatment Center (NIH P30 CA118100).

ABBREVIATIONS USED

MC1	melanocortin-1
α-MSH	α-melanocyte stimulating hormone
RGD motif	Arg-Gly-Asp-ᴅTyr-Asp
MS	mass spectrometry
SPECT	single photon emission computed tomography
Pbf	2,2,4,6,7-pentamethyl-dihydrobenzofurane-5-sulfonyl
tBu	tertiary butyl
Boc	tertiary-butyloxycarbonyl
Trt	trityl
PyBOP	benzotriazole-1-yl-oxy-tris-pyrrolidino-phosphonium-hexafluorophosphate
DIPEA	N,N-diisopropylethylamine

REFERENCES

1. Siegel R, Naishadham D, Jemal A. Cancer Statistics, 2013. CA Cancer J. Clin. 2013; 63:11–30. [PubMed: 23335087]
2. Giblin MF, Wang N, Hoffman TJ, Jurisson SS, Quinn TP. Design and characterization of alpha-melanotropin peptide analogs cyclized through rhenium and technetium metal coordination. Proc. Natl. Acad. Sci. USA. 1998; 95:12814–12818. [PubMed: 9788997]
3. Froidevaux S, Calame-Christe M, Tanner H, Sumanovski L, Eberle AN. A novel DOTA-alpha-melanocyte-stimulating hormone analog for metastatic melanoma diagnosis. J. Nucl. Med. 2002; 43:1699–1706. [PubMed: 12468522]
4. Miao Y, Whitener D, Feng W, Owen NK, Chen J, Quinn TP. Evaluation of the human melanoma targeting properties of radiolabeled alpha-melanocyte stimulating hormone peptide analogues. Bioconjug. Chem. 2003; 14:1177–1184. [PubMed: 14624632]

5. Froidevaux S, Calame-Christe M, Schuhmacher J, Tanner H, Saffrich R, Henze M, Eberle AN. A Gallium-labeled DOTA-α-melanocyte-stimulating hormone analog for PET imaging of melanoma metastases. J. Nucl. Med. 2004; 45:116–123. [PubMed: 14734683]
6. McQuade P, Miao Y, Yoo J, Quinn TP, Welch MJ, Lewis JS. Imaging of melanoma using ^{64}Cu- and ^{86}Y-DOTA-ReCCMSH(Arg^{11}), a cyclized peptide analogue of alpha-MSH. J. Med. Chem. 2005; 48:2985–2992. [PubMed: 15828837]
7. Wei L, Butcher C, Miao Y, Gallazzi F, Quinn TP, Welch MJ, Lewis JS. Synthesis and biologic evaluation of ^{64}Cu-labeled rhenium-cyclized alpha-MSH peptide analog using a cross-bridged cyclam chelator. J. Nucl. Med. 2007; 48:64–72. [PubMed: 17204700]
8. Cheng Z, Xiong Z, Subbarayan M, Chen X, Gambhir SS. ^{64}Cu-labeled alpha-melanocyte-stimulating hormone analog for MicroPET imaging of melanocortin 1 receptor expression. Bioconjug. Chem. 2007; 18:765–772. [PubMed: 17348700]
9. Miao Y, Benwell K, Quinn TP. ^{99m}Tc- and ^{111}In-labeled alpha-melanocyte-stimulating hormone peptides as imaging probes for primary and pulmonary metastatic melanoma detection. J. Nucl. Med. 2007; 48:73–80. [PubMed: 17204701]
10. Miao Y, Figueroa SD, Fisher DR, Moore HA, Testa RF, Hoffman TJ, Quinn TP. ^{203}Pb-labeled alpha-melanocyte-stimulating hormone peptide as an imaging probe for melanoma detection. J. Nucl. Med. 2008; 49:823–829. [PubMed: 18413404]
11. Miao Y, Gallazzi F, Guo H, Quinn TP. ^{111}In-labeled lactam bridge-cyclized alpha-melanocyte stimulating hormone peptide analogues for melanoma imaging. Bioconjug. Chem. 2008; 19:539–547. [PubMed: 18197608]
12. Guo H, Shenoy N, Gershman BM, Yang J, Sklar LA, Miao Y. Metastatic melanoma imaging with an ^{111}In-labeled lactam bridge-cyclized alpha-melanocyte-stimulating hormone peptide. Nucl. Med. Biol. 2009; 36:267–276. [PubMed: 19324272]
13. Guo H, Yang J, Gallazzi F, Miao Y. Reduction of the ring size of radiolabeled lactam bridge-cyclized alpha-MSH peptide resulting in enhanced melanoma uptake. J. Nucl. Med. 2010; 51:418–426. [PubMed: 20150256]
14. Guo H, Yang J, Gallazzi F, Miao Y. Effects of the amino acid linkers on melanoma-targeting and pharmacokinetic properties of Indium-111-labeled lactam bridge-cyclized α-MSH peptides. J. Nucl. Med. 2011; 52:608–616. [PubMed: 21421725]
15. Haubner R, Wester HJ, Reuning U, Senekowitsch-Schmidtke R, Diefenbach B, Kessler H, Stöcklin G, Schwaiger M. Radiolabeled alpha(v)beta(3) integrin antagonists: a new class of tracers for tumor targeting. J. Nucl. Med. 1999; 40:1061–1071. [PubMed: 10452325]
16. Poethko T, Schottelius M, Thumshirn G, Hersel U, Herz M, Henriksen G, Kessler H, Schwaiger M, Wester HJ. Two-step methodology for high-yield routine radiohalogenation of peptides: ^{18}F-labeled RGD and octreotide analogs. J. Nucl. Med. 2004; 45:892–902. [PubMed: 15136641]
17. Li C, Wang W, Wu Q, Ke S, Houston J, Sevick-Muraca E, Dong L, Chow D, Charnsangavej C, Gelovani JG. Dual optical and nuclear imaging in human melanoma xenografts using a single targeted imaging probe. Nucl. Med. Biol. 2006; 33:349–358. [PubMed: 16631083]
18. Decristoforo C, Faintuch-Linkowski B, Rey A, von Guggenberg E, Rupprich M, Hernandez-Gonzales I, Rodrigo T, Haubner R. [^{99m}Tc]HYNIC-RGD for imaging integrin alphavbeta3 expression. Nucl. Med. Biol. 2006; 33:945–952. [PubMed: 17127166]
19. Alves S, Correia JD, Gano L, Rold TL, Prasanphanich A, Haubner R, Rupprich M, Alverto R, Decristoforo C, Santos I, Smith CJ. In vitro and in vivo evaluation of a novel ^{99m}Tc(CO)$_3$-pyrazolyl conjugate of cyclo-(Arg-Gly-Asp-d-Tyr-Lys). Bioconjug. Chem. 2007; 18:530–537. [PubMed: 17373771]
20. Decristoforo C, Hernandez Gonzalez I, Carlsen J, Rupprich M, Huisman M, Virgolini I, Wester HJ, Haubner R. ^{68}Ga- and ^{111}In-labelled DOTA-RGD peptides for imaging of alpha(v)beta(3) integrin expression. Eur. J. Nucl. Med. Mol. Imaging. 2008; 35:1507–1515. [PubMed: 18369617]
21. Hultsch C, Schottelius M, Auernheimer J, Alke A, Wester HJ. ^{18}F-Fluoroglucosylation of peptides, exemplified on cyclo(RGDfK). Eur. J. Nucl. Med. Mol. Imaging. 2009; 36:1469–1474. [PubMed: 19350236]

22. Wei L, Ye Y, Wadas TJ, Lewis JS, Welch MJ, Achilefu S, Anderson CJ. ^{64}Cu-labeled CB-TE2A and diamsar-conjugated RGD peptide analogs for targeting angiogenesis: comparison of their biological activity. Nucl. Med. Biol. 2009; 36:277–285. [PubMed: 19324273]

23. Yang J, Guo H, Miao Y. Technetium-99m-labeled Arg-Gly-Asp-conjugated alpha-melanocyte stimulating hormone hybrid peptides for human melanoma imaging. Nucl. Med. Biol. 2010; 37:873–883. [PubMed: 21055617]

24. Yang J, Miao Y. Substitution of Gly with Ala enhanced the melanoma uptake of technetium-99m-labeled Arg-Ala-Asp-conjugated alpha-melanocyte stimulating hormone peptide. Bioorg. Med. Chem. Lett. 2012; 22:1541–1545. [PubMed: 22297112]

25. Flook AM, Yang J, Miao Y. Evaluation of new Tc-99m-labeled Arg-X-Asp-conjugated alpha-melanocyte stimulating hormone peptides for melanoma imaging. Mol. Pharmaceutics. 2013; 10:3417–3424.

26. Yang J, Guo H, Gallazzi F, Berwick M, Padilla RS, Miao Y. Evaluation of a novel RGD-conjugated alpha-melanocyte stimulating hormone hybrid peptide for potential melanoma therapy. Bioconjug. Chem. 2009; 20:1634–1642. [PubMed: 19552406]

27. Miao Y, Owen NK, Whitener D, Gallazzi F, Hoffman TJ, Quinn TP. In vivo evaluation of ^{188}Re-labeled alpha-melanocyte stimulating hormone peptide analogs for melanoma therapy. Int. J. Cancer. 2002; 101:480–487. [PubMed: 12216078]

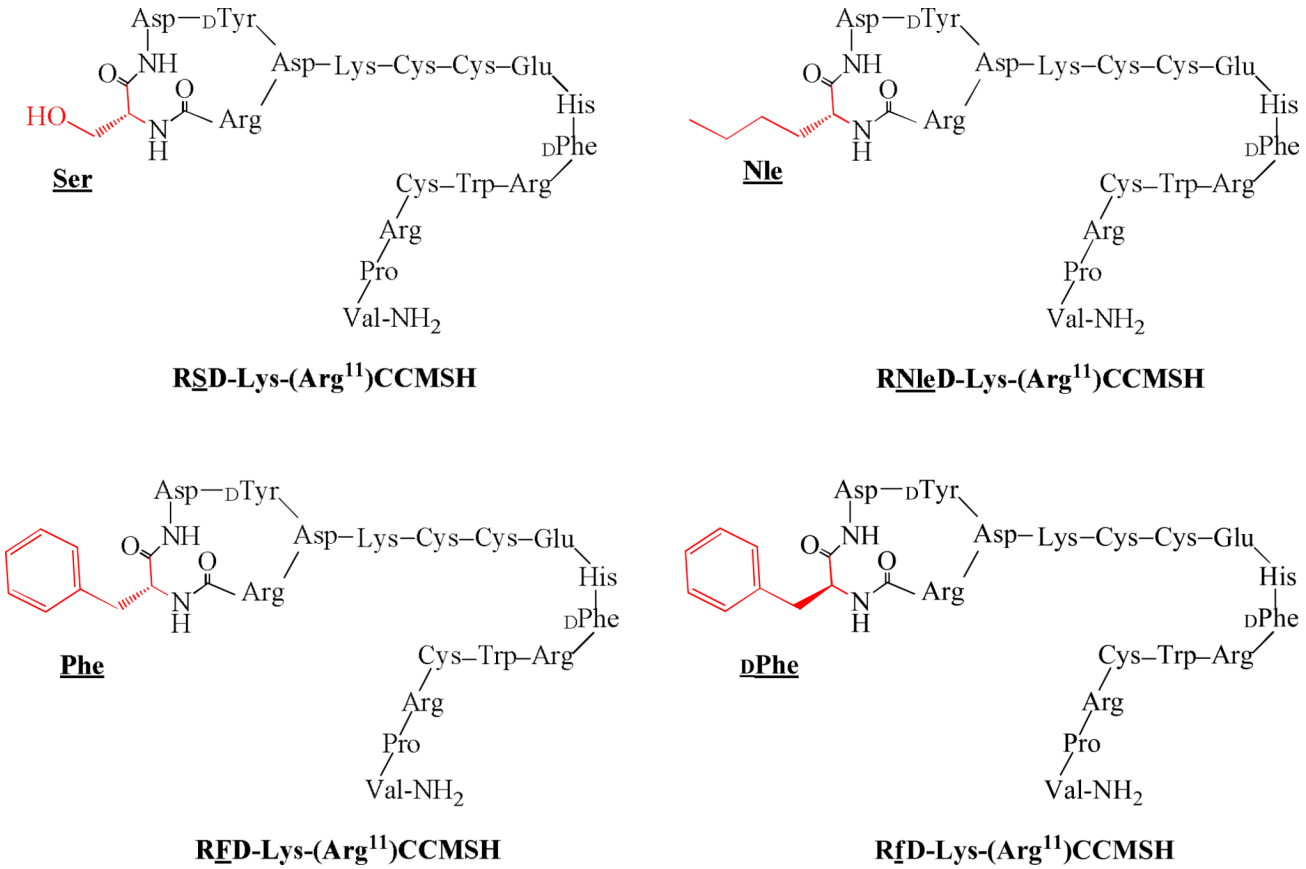

Figure 1.
Schematic structures of RXD-Lys-(Arg^{11})CCMSH peptides.

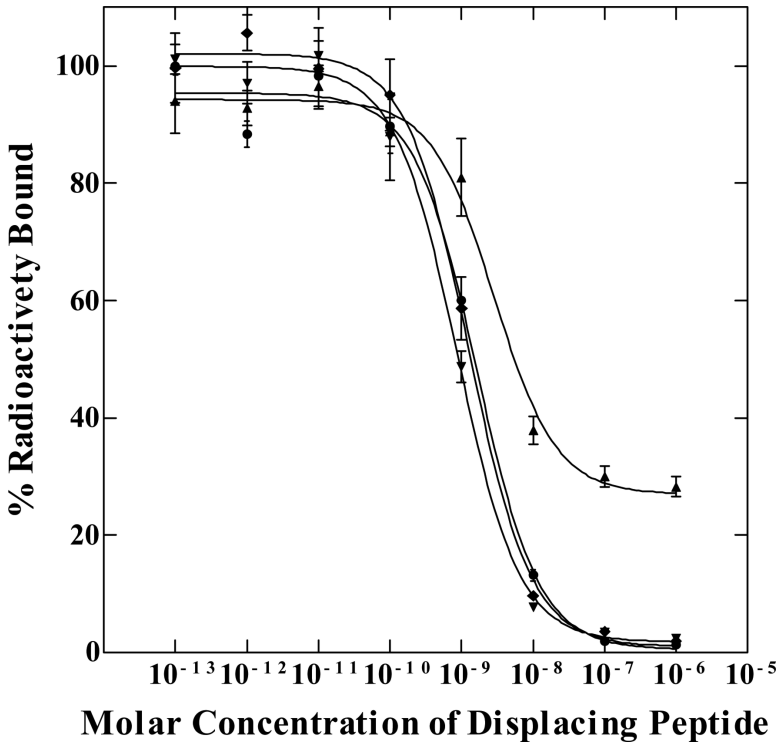

Figure 2.

The competitive binding curves of RSD-Lys-(Arg^{11})CCMSH (●), RNleD-Lys-(Arg^{11})CCMSH (▲), RFD-Lys-(Arg^{11})CCMSH (■), and RfD-Lys-(Arg^{11})CCMSH (◆) in B16/F1 murine melanoma cells. The IC_{50} value was 1.30 ± 0.36 nM for RSD-Lys-(Arg^{11})CCMSH, 2.99 ± 0.26 nM for RNleD-Lys-(Arg^{11})CCMSH, 0.82 ± 0.06 nM for RFD-Lys-(Arg^{11})CCMSH, and 1.35 ± 0.08 nM for RfD-Lys-(Arg^{11})CCMSH, respectively.

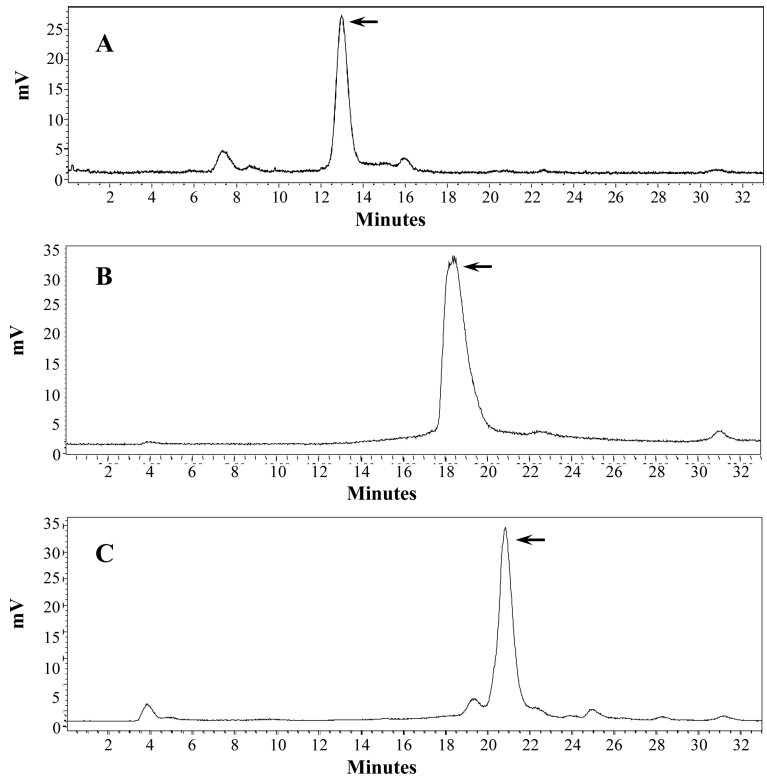

Figure 3.

Radioactive HPLC profiles of ^{99m}Tc-RSD-Lys-(Arg^{11})CCMSH (A), ^{99m}Tc-RFD-Lys-(Arg^{11})CCMSH (B) and ^{99m}Tc-RfD-Lys-(Arg^{11})CCMSH (C) in mouse serum after incubation at 37 °C for 24 h. The arrows denote the original retention times of ^{99m}Tc-RSD-Lys-(Arg^{11})CCMSH (12.5 min), ^{99m}Tc-RFD-Lys-(Arg^{11})CCMSH (18.4 min) and ^{99m}Tc-RfD-Lys-(Arg^{11})CCMSH (20.8 min) prior to the incubation in mouse serum.

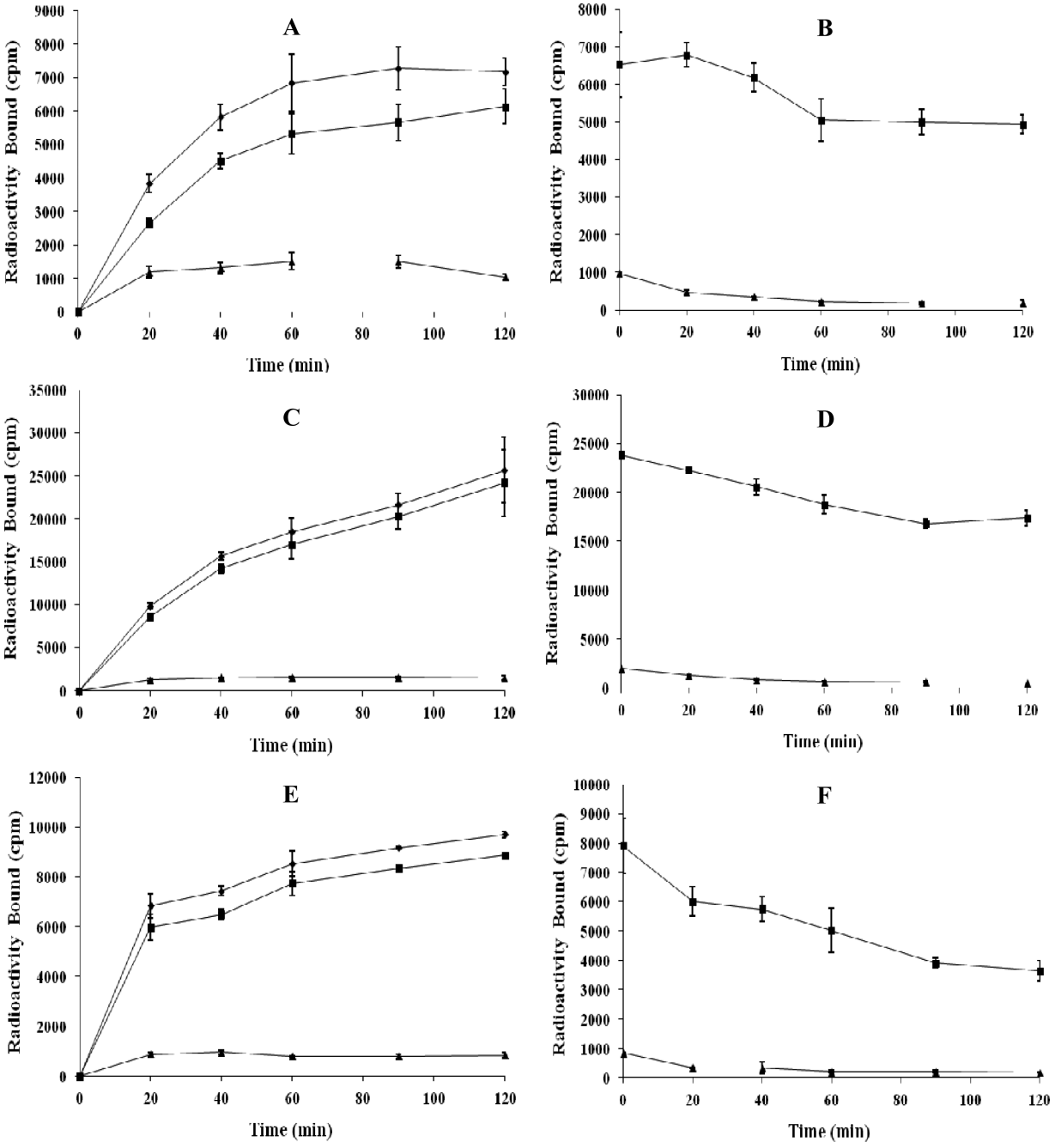

Figure 4.

Cellular internalization and efflux of ^{99m}Tc-RSD-Lys-(Arg^{11})CCMSH (A and B), ^{99m}Tc-RFD-Lys-(Arg^{11})CCMSH (C and D) and ^{99m}Tc-RfD-Lys-(Arg^{11})CCMSH (E and F) in B16/F1 melanoma cells. Total bound radioactivity (◆), internalized radioactivity (■) and cell membrane radioactivity (▲) were presented as counts per minute (cpm).

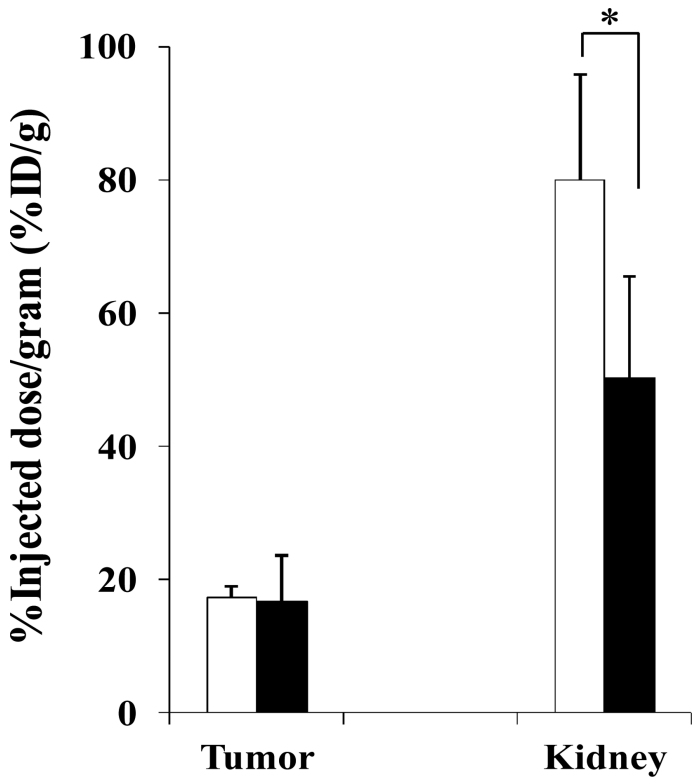

Figure 5.

Effect of *L*-lysine co-injection on the tumor and kidney uptakes of ^{99m}Tc-RSD-Lys-(Arg^{11})CCMSH at 2 h post-injection in B16/F1 melanoma-bearing C57 mice. The white (□) and black (■) columns represent the tumor and renal uptake of ^{99m}Tc-RSD-Lys-(Arg^{11})CCMSH with or without *L*-lysine co-injection. *L*-lysine co-injection significantly (*$p<0.05$) reduced the renal uptake of ^{99m}Tc-RSD-Lys-(Arg^{11})CCMSH by 37% at 2 h post-injection without affecting the tumor uptake.

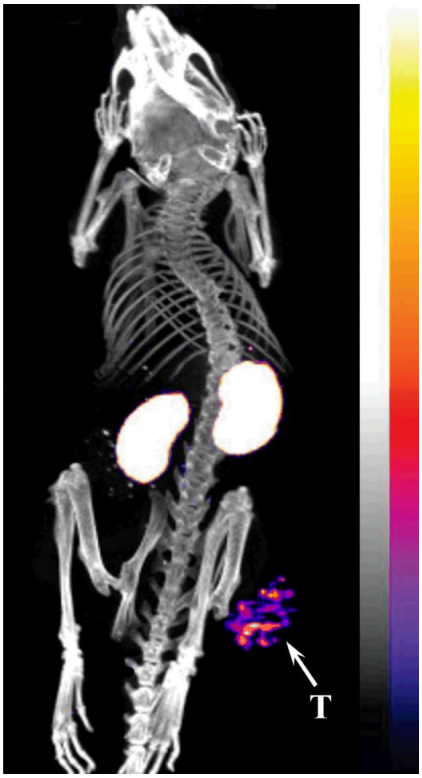

Figure 6.
Representative whole-body SPECT/CT image of B16/F1 melanoma- bearing C57 mice 2 h post injection of 7.4 MBq of ^{99m}Tc-RSD-Lys-(Arg^{11})CCMSH. Flank melanoma lesions (T) are highlighted with an arrow on the image.

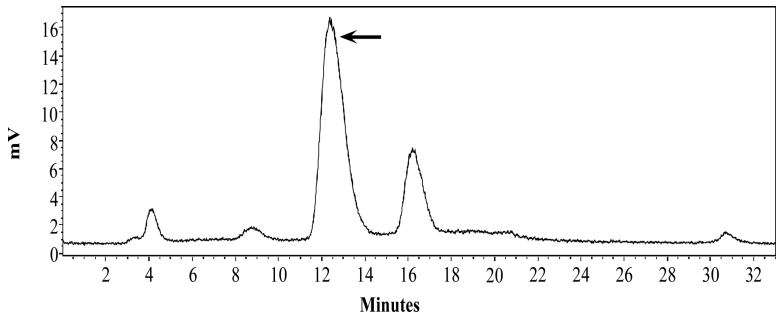

Figure 7.
Radioactive HPLC profiles of urinary metabolites at 2 h post-injection of ^{99m}Tc-RSD-Lys-(Arg^{11})CCMSH. The arrow denotes the original retention time of ^{99m}Tc-RSD-Lys-(Arg^{11})CCMSH (12.5 min) prior to tail vein injection.

Table 1

Capacity factors, chemical/radiochemical purities and measured molecular weights of RXD-Lys-(Arg^{11})CCMSH peptides and their ^{99m}Tc-conjugates.

	Capacity factor (k')	Chemical/Radiochemical Purity (%)	Measured Molecular Weight (Da)
RSD-Lys-(Arg^{11})CCMSH	2.19	97.01	2180
RNleD-Lys-(Arg^{11})CCMSH	4.36	95.83	2206
RFD-Lys-(Arg^{11})CCMSH	3.77	98.25	2240
RfD-Lys-(Arg^{11})CCMSH	3.86	95.75	2240
^{99m}Tc-RSD-Lys-(Arg^{11})CCMSH	3.18	99.75	ND
^{99m}Tc-RFD-Lys-(Arg^{11})CCMSH	4.93	99.27	ND
^{99m}Tc-RfD-Lys-(Arg^{11})CCMSH	5.13	99.78	ND

ND = not determined.

Table 2

Biodistribution of ^{99m}Tc-RSD-Lys-(Arg^{11})CCMSH in B16/F1 melanoma-bearing C57 mice. The data was presented as percent injected dose/gram or as percent injected dose (mean ± SD, n=4).

Tissue	0.5 h	2 h	4 h	24 h	2 h NDP Blockade
			Percent injected dose/gram (%ID/g)		
Tumor	18.01 ± 4.22	17.42 ± 1.52	10.12 ± 1.72	8.04 ± 1.80	2.35 ± 0.01*
Brain	0.25 ± 0.12	0.02 ± 0.01	0.01 ± 0.01	0.06 ± 0.01	0.05 ± 0.01
Blood	13.59 ± 1.25	0.19 ± 0.11	0.06 ± 0.04	2.01 ± 1.52	0.69 ± 0.42
Heart	2.14 ± 0.49	0.14 ± 0.05	0.09 ± 0.04	0.14 ± 0.05	0.46 ± 0.30
Lung	3.69 ± 1.18	0.33 ± 0.13	0.22 ± 0.06	0.27 ± 0.13	0.65 ± 0.16
Liver	2.25 ± 0.20	1.22 ± 0.12	1.57 ± 0.81	0.70 ± 0.14	1.54 ± 0.11
Skin	5.31 ± 0.63	0.33 ± 0.10	0.27 ± 0.05	2.19 ± 0.58	0.75 ± 0.02
Spleen	1.73 ± 0.17	0.18 ± 0.10	0.38 ± 0.15	0.22 ± 0.07	0.28 ± 0.10
Stomach	2.31 ± 0.31	0.73 ± 0.08	0.61 ± 0.18	0.30 ± 0.17	1.19 ± 0.04
Kidneys	98.25 ± 13.78	80.01 ± 15.67	69.23 ± 17.41	23.15 ± 2.94	90.41 ± 19.21
Muscle	1.42 ± 0.57	0.09 ± 0.04	0.07 ± 0.04	1.01 ± 0.50	0.09 ± 0.06
Pancreas	0.68 ± 0.27	0.04 ± 0.04	0.09 ± 0.06	0.17 ± 0.07	0.15 ± 0.03
Bone	2.11 ± 0.67	0.44 ± 0.18	0.32 ± 0.19	0.59 ± 0.09	0.47 ± 0.13
			Percent injected dose (%ID)		
Intestines	2.02 ± 0.17	0.63 ± 0.08	1.48 ± 0.22	0.66 ± 0.27	1.06 ± 0.79
Urine	36.01 ± 2.73	68.19 ± 9.80	74.72 ± 6.63	84.03 ± 2.67	69.99 ± 4.72
			Uptake ratio of tumor/normal tissue		
Tumor/Blood	1.33	91.68	168.67	4.02	3.41
Tumor/Kidneys	0.18	0.22	0.15	0.35	0.03
Tumor/Lung	4.88	52.79	46.00	29.78	3.62
Tumor/Liver	8.00	14.28	6.45	11.49	1.53
Tumor/Muscle	12.68	193.56	144.57	8.04	26.11

*$p<0.05$ ($p=0.002$) for determining the significance of differences in tumor and kidney uptake between ^{99m}Tc-RSD-Lys-(Arg^{11})CCMSH with or without NDP-MSH peptide blockade at 2 h post-injection.

Table 3

Biodistribution of ^{99m}Tc-RFD-Lys-(Arg^{11})CCMSH in B16/F1 melanoma-bearing C57 mice. The data was presented as percent injected dose/gram or as percent injected dose (mean ± SD, n=4).

Tissue	0.5 h	2 h	4 h	24 h	2 h NDP Blockade
			Percent injected dose/gram (%ID/g)		
Tumor	7.42 ± 3.56	11.22 ± 1.53	13.11 ± 1.21	6.29 ± 1.39	1.57 ± 0.48*
Brain	0.21 ± 0.01	0.07 ± 0.01	0.04 ± 0.01	0.01 ± 0.01	0.08 ± 0.01
Blood	6.78 ± 3.79	1.99 ± 0.24	0.91 ± 0.38	0.23 ± 0.01	1.61 ± 0.01
Heart	2.63 ± 1.13	0.94 ± 0.11	0.88 ± 0.35	0.14 ± 0.02	0.76 ± 0.17
Lung	7.51 ± 1.60	3.38 ± 0.48	2.11 ± 0.51	0.38 ± 0.17	2.10 ± 0.29
Liver	6.75 ± 2.44	9.87 ± 1.26	12.11 ± 1.86	4.73 ± 1.53	6.34 ± 2.19
Skin	4.27 ± 1.16	1.54 ± 0.20	0.87 ± 0.17	0.46 ± 0.05	1.48 ± 0.44
Spleen	4.82 ± 1.31	4.40 ± 0.72	4.85 ± 1.33	2.56 ± 0.45	2.40 ± 1.11
Stomach	6.21 ± 0.37	4.40 ± 3.33	3.80 ± 1.14	0.92 ± 0.44	10.65 ± 2.76
Kidneys	56.86 ± 16.58	88.08 ± 9.31	81.89 ± 23.37	51.01 ± 3.62	72.29 ± 6.08
Muscle	1.27 ± 0.42	0.31 ± 0.19	0.21 ± 0.01	0.01 ± 0.01	0.33 ± 0.15
Pancreas	1.17 ± 0.23	0.38 ± 0.17	0.45 ± 0.01	0.20 ± 0.08	0.19 ± 0.08
Bone	1.97 ± 0.32	1.11 ± 0.07	0.44 ± 0.25	0.41 ± 0.25	0.05 ± 0.01
			Percent injected dose (%ID)		
Intestines	3.23 ± 1.73	4.69 ± 1.24	7.02 ± 2.79	1.50 ± 0.50	13.77 ± 11.25
Urine	30.19 ± 11.73	42.61 ± 2.89	61.42 ± 0.29	75.8 ± 5.02	39.05 ± 10.35
			Uptake ratio of tumor/normal tissue		
Tumor/Blood	1.09	5.64	14.41	27.35	0.98
Tumor/Kidneys	0.13	0.13	0.16	0.12	0.02
Tumor/Lung	0.99	3.38	6.21	16.55	0.75
Tumor/Liver	1.10	1.14	1.08	1.33	0.25
Tumor/Muscle	5.84	36.19	62.43	629.00	4.76

* $p<0.05$ ($p=0.001$) for determining the significance of differences in tumor and kidney uptake between ^{99m}Tc-RFD-Lys-(Arg^{11})CCMSH with or without NDP-MSH peptide blockade at 2 h post-injection.

Table 4

Biodistribution of ^{99m}Tc-RfD-Lys-(Arg^{11})CCMSH in B16/F1 melanoma-bearing C57 mice. The data was presented as percent injected dose/gram or as percent injected dose (mean ± SD, n=4).

Tissue	0.5 h	2 h	4 h	24 h	2 h NDP Blockade
			Percent injected dose/gram (%ID/g)		
Tumor	9.56 ± 2.36	12.68 ± 2.39	15.01 ± 4.40	7.19 ± 1.02	2.82 ± 0.48*
Brain	0.16 ± 0.01	0.04 ± 0.01	0.03 ± 0.02	0.01 ± 0.01	0.04 ± 0.01
Blood	7.85 ± 2.12	1.01 ± 0.11	0.45 ± 0.12	0.06 ± 0.01	0.74 ± 0.01
Heart	2.67 ± 0.89	0.50 ± 0.17	0.45 ± 0.12	0.21 ± 0.08	0.60 ± 0.09
Lung	6.44 ± 1.81	2.73 ± 1.08	1.19 ± 0.44	0.47 ± 0.22	1.83 ± 0.35
Liver	6.59 ± 0.61	5.29 ± 1.30	4.47 ± 1.63	4.57 ± 0.45	3.77 ± 1.53
Skin	4.87 ± 0.41	1.25 ± 0.29	0.85 ± 0.11	0.34 ± 0.08	1.30 ± 0.43
Spleen	2.98 ± 1.23	1.26 ± 0.45	0.86 ± 0.19	0.76 ± 0.08	0.93 ± 0.36
Stomach	3.37 ± 1.40	2.71 ± 0.75	1.86 ± 0.46	0.51 ± 0.11	4.49 ± 0.85
Kidneys	103.75 ± 11.26	111.54 ± 10.19	104.95 ± 8.06	73.05 ± 9.87	111.34 ± 12.41
Muscle	0.45 ± 0.12	0.04 ± 0.03	0.02 ± 0.01	0.04 ± 0.03	0.03 ± 0.01
Pancreas	0.48 ± 0.16	0.38 ± 0.15	0.18 ± 0.03	0.05 ± 0.01	0.31 ± 0.11
Bone	0.07 ± 0.06	0.43 ± 0.07	0.15 ± 0.03	0.19 ± 0.14	0.38 ± 0.30
			Percent injected dose (%ID)		
Intestines	2.49 ± 0.60	2.58 ± 1.38	3.18 ± 1.08	0.82 ± 0.14	2.65 ± 1.53
Urine	22.56 ± 12.86	44.49 ± 12.39	50.50 ± 8.66	72.74 ± 7.36	54.88 ± 2.72
			Uptake ratio of tumor/normal tissue		
Tumor/Blood	1.22	12.55	33.36	119.83	3.81
Tumor/Kidneys	0.09	0.11	0.14	0.10	0.03
Tumor/Lung	1.48	4.64	12.61	15.30	1.54
Tumor/Liver	1.45	2.40	3.36	1.57	0.75
Tumor/Muscle	21.24	317.00	750.50	179.75	94.00

*$p<0.05$ ($p=0.002$) for determining the significance of differences in tumor and kidney uptake between ^{99m}Tc-RfD-Lys-(Arg^{11})CCMSH with or without NDP-MSH peptide blockade at 2 h post-injection.